

Observations of Wind-generated Shoreface Currents off Duck, North Carolina

J.P. Xu†§ and L.D. Wright‡

† Coastal Morphodynamics
Laboratory
Louisiana State University
Baton Rouge, LA 70803, USA

‡ School of Marine Science
Virginia Institute of Marine
Science
College of William and Mary
Gloucester Point, VA 23062,
USA

ABSTRACT

XU, J.P. and WRIGHT, L.D., 1998. Observations of wind-generated shoreface currents off Duck, North Carolina. *Journal of Coastal Research*, 14(2), 610-619. Royal Palm Beach (Florida), ISSN 0749-0208.

Wind, wave and currents measurements at 9 and 14 meter water depths on the shoreface off U.S. Army Corps of Engineers Field Research Facility at Duck, North Carolina are presented. Coastal setup accompanied by southerly-setting alongshore currents and seaward cross-shore currents is developed during Northeasterly storms. Coastal set-down, with reversal currents, is generated by Southerly or southwesterly strong winds. However, while the current speed during Northeasterly storms is strongly correlated with the wind stress, this relationship does not hold during Southwesterly storms. This is attributable to the fact that downwelling-favorable Northeasterlies enhance the coastal jet and act to reinforce the coastal plume that often issues from the Chesapeake Bay.

ADDITIONAL INDEX WORDS: *Wind waves, shoreface currents, wind stress.*



INTRODUCTION

Off a wave dominated sandy coast, the shoreface is a region of concave-upward bottom slope lying between the outreaches of the surf zone and the inner continental shelf (NIEDORODA *et al.*, 1984). In this transition zone, interactions between shelf processes dominated by the large-scale circulation and surf zone processes dominated by radiation stress gradients associated with breaking waves produce a unique and complicated dynamic environment. This regime plays an important role in cross-shore and alongshore sediment transport. In the past decade, the development of oceanographic instruments and their use in shoreface and inner continental shelf studies have significantly expanded our knowledge (BOWEN, 1980; CSANADY, 1982; GUZA and THORNTON, 1985; HEQUETTE and HILL, 1993; NIEDORODA *et al.*, 1985; SWIFT *et al.*, 1985; WRIGHT *et al.*, 1986; WRIGHT *et al.*, 1994). In an experiment off Tiana Beach, Long Island, NIEDORODA *et al.* (1984, 1985) studied the shoreface morphodynamics on a wavedominated coast and thoroughly documented the relationships between wind, shoreface currents (downwelling, upwelling) and shoreface sediment transport. WRIGHT *et al.*, (1991) analyzed 3 years of data collected under storm, fair weather and swell-dominated conditions from Duck, North Carolina shoreface and compared the contribution to the cross-shore sediment transport made by mean-currents, gravity waves, and infragravity waves. The results showed that mean-flow played the most important role, especially during

storms, in cross-shore sediment transport. Subsequent studies confirmed this conclusion (WRIGHT *et al.*, 1994). HEQUETTE and HILL (1993) described storm-generated shoreface circulation on Tibjak Beach, Canadian Beaufort Sea and also indicated the strong, but complex relationship between current, sediment transport and winds. In this paper, we report the results from a field deployment of two instrumented tetrapods on the shoreface off Duck, North Carolina. The relationships between wind, and wind-generated waves and currents under both storm and calm inter-storm conditions are qualitatively evaluated.

STUDY SITE AND FIELD DATA

Field data were obtained on the inner shelf seaward of the U.S. Army Corps of Engineers Field Research Facility (FRF) at Duck, North Carolina in the southern part of the Middle Atlantic Bight, 36°07'N; 75°39'W, (Figure 1). Two instrumented tetrapods (WRIGHT *et al.*, 1991; WRIGHT *et al.*, 1994) were deployed at water depths of 9 m (hereafter inshore site) and 14 m (hereafter offshore site) during October 28 to November 23, 1992. The offshore tetrapod had an array of 5 optical backscatter sensors, an array of 4 Marsh-McBirney current meters (at 10, 40, 70, and 100 cm above bottom respectively), and a directional wave gauge (a pressure sensor, located at 260 cm above bottom, and a 2-axis Marsh-McBirney current meter). The inshore tetrapod consisted of an array of five optical backscatter sensors and one directional wave gauge, whose pressure sensor was at 250 cm above bottom and current meter at 17 cm above bottom respectively. Except for the directional wave gauge on the offshore pod that sampled 4,096 data points at a sampling rate of 5 Hz

95085 received 16 July 1995; accepted in revision 3 July 1997.

§Present address: U.S. Geological Survey, 345 Middlefield Road, MS-999, Menlo Park, CA 94025, U.S.A.

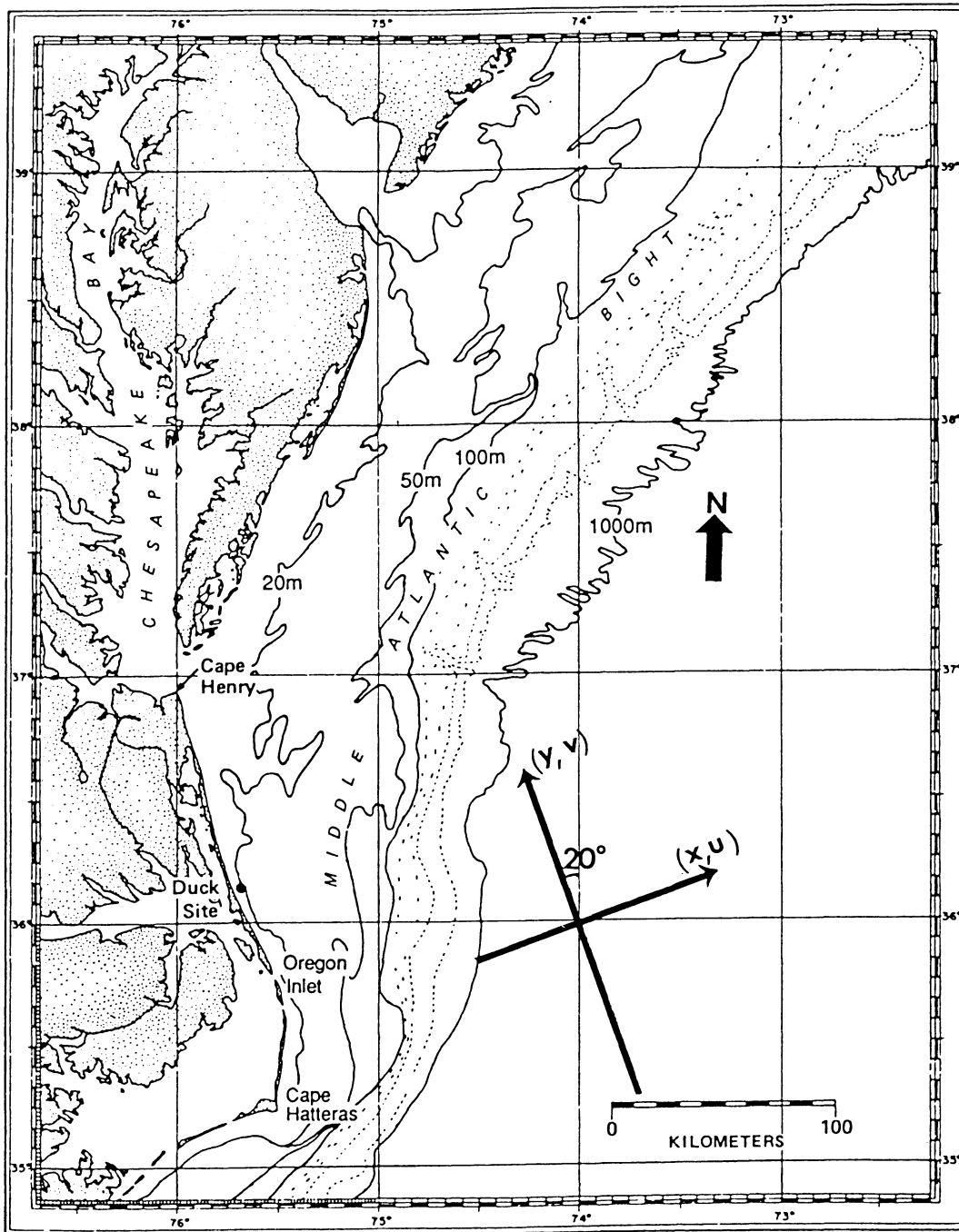


Figure 1. Location map of study site.

every 3 hours, all other sensors were set to sample 2,048 data points at 1 Hz sampling rate every 3 hours. In addition to data from the tetrapod, burst-mean wave and current data obtained from FRF's PUV gauge deployed at 6 meter of water depth are also used. Wind data, also burst-averaged, were collected at the end of the FRF pier. Because of the different sampling scheme between our tetrapods and FRF's instru-

ments, which samples 1,024 points at a rate of 1 Hz every 34 minutes), FRF's wind data had to be interpolated when used with the tetrapod data. Except for the data of one current meter (at 40 cm above bottom) from the offshore pod that were corrupted for unknown reasons, the data from all other sensors were of good quality, and are used in the evaluation and discussion that follow.

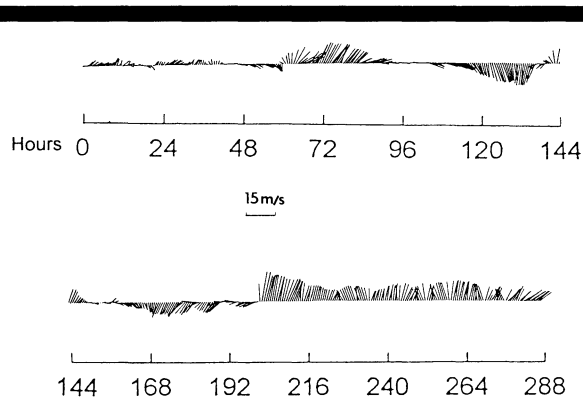


Figure 2. Stick plot of winds measured at the end of U.S. Army Corps of Engineers, Field Research Facility's research pier at Duck, North Carolina. Hour 0 is 12:00 PM, October 28, 1992.

RESULTS

The field data were analyzed to obtain the burst-mean direction and speed of winds and currents, significant wave height and peak wave period (WRIGHT *et al.*, 1991). The horizontal Cartesian coordinates were rotated in such a way that the x component is perpendicular to the shoreline, which is about 20° from the true North-South (Figure 1). Throughout this paper, all directions are defined according to the rotated coordinates, *e.g.* currents with direction of 270° will be perpendicular toward the shoreline (negative and shoreward), and a 90° current will be positive and seaward.

During the 12 days deployment, Northeasterly winds dominated at the sites. Among them were two "Northeasters" (WRIGHT *et al.*, 1986) that passed through the area on October 31 and November 6, 1992 respectively (Figure 2). During the first "Northeaster", strong NE winds with speeds over 10 m/s blew for at least 10 hours. The second "Northeaster" storm brought even stronger NNE winds (15 m/s). The most significant difference between the two storms, however, were what followed them. After the November 6 storm, weaker NNE and NNW winds with speeds of 5 ~ 10 m/s continued blowing for over 70 hours until the end of the deployment. When the October 31 storm subsided, it was followed by fairly strong Southeasterly winds for more than 24 hours.

The observed wave conditions showed strong correlation with the winds, especially during the two storms. The significant wave height, peak wave period and wave direction from the Field Research Facility PUV gage are plotted in Figure 3. Prior to the first storm, conditions were relatively calm (significant wave height, $H_{mo} < 0.5$ m) and long period waves (probably swell) propagated in a direction approximately normal to shore. When the October 31 storm began (Hr. 66), locally generated high seas ($H_{mo} > 1.5$ m) dominated; peak wave period dropped abruptly from 13 seconds to as low as 5 seconds; and wave direction shifted and aligned with the wind which was blowing toward the SW.

The variations of wave height, period and direction were also clearly demonstrated during the second storm on November 6 (Hr. 204). Similar to the relatively calm period prior to the first storm, the inter-storm time period was repre-

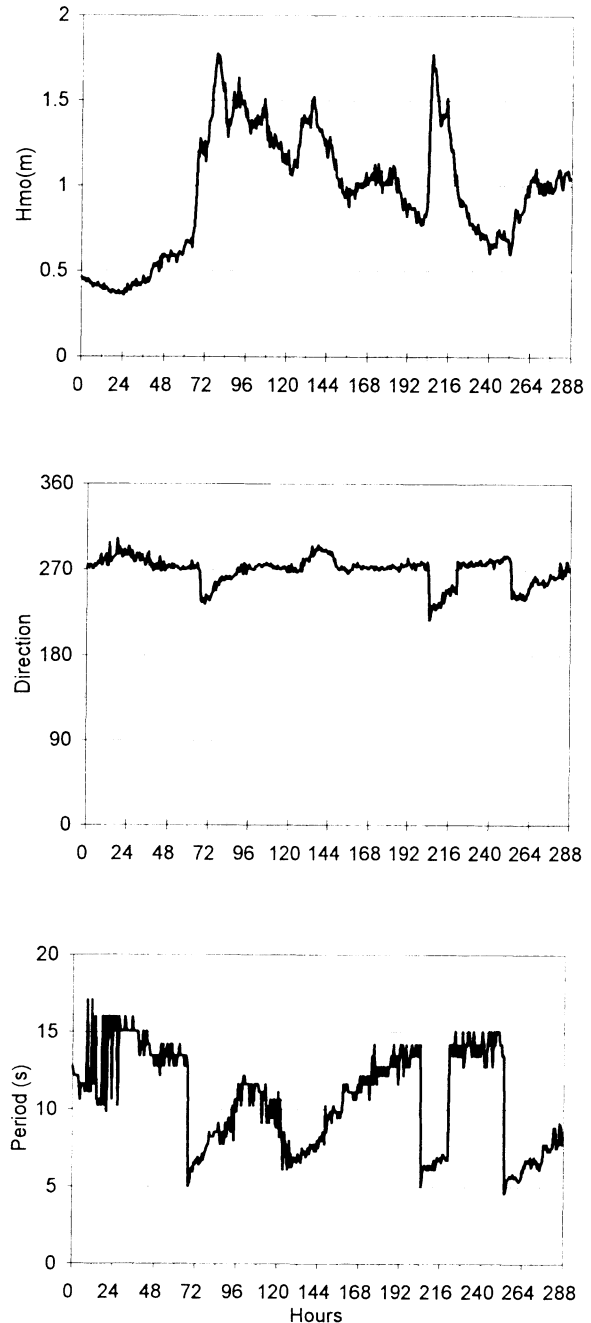


Figure 3. Significant wave height, wave direction and period recorded from FRF's PUV gage at depth of 6 m. Hour 0 is 12:00 PM, October 28, 1992.

sented by long period waves travelling normally toward the shoreline except the November 3 (Hr. 144) strong wind event in which strong Southwesterly winds blew over 12 hours. In Figure 4, the power spectral density of three bursts (Hr. 48 for pre-storm, Hr. 64 for storm, and Hr. 120 for post-storm conditions) are plotted. At both offshore and inshore sites, the pre-storm condition was represented by long period (13 sec-

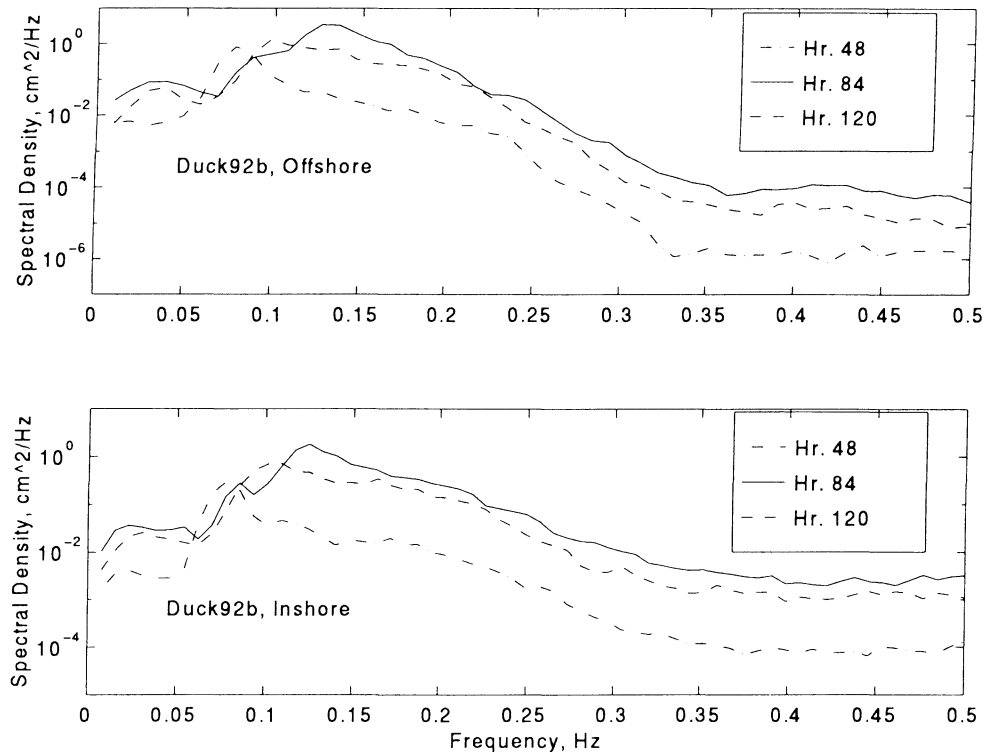


Figure 4. Power spectral density of surface waves for the three bursts that represent pre-storm, storm, and post-storm conditions during the Oct. 31 storm, at the offshore site (upper panel) and the inshore site (lower panel).

ond) swell. During the storm, the wind-wave energy increased, almost by one order of magnitude at the inshore site and 3 times at the offshore, and overwhelmed the existing swells whose energy decreased a small amount. Swell again became dominant following the storm. A similar pattern characterized the second storm (Figure 5). The distinction between this storm and the first one is that the swell and sea wave during the second storm were further apart in frequency bands and the swell, which had considerable energy, coexisted with the waves.

All strong current events measured at the three locations were storm-induced. There were relatively weak tidal flows but they were overwhelmed by the much stronger wind-induced components during the storms. Figures 6, 7 and 8 display the burst-mean cross-shore, u , and alongshore, v , current velocity and direction along with the direction of the wind. Prior to the first Northeaster storm, the mean currents were weak, both cross-shore and alongshore components exhibited tidally (semi-diurnal) induced fluctuations. The two strong pulses of the southerly-setting alongshore (v) components were apparently generated by the Northeasters. The v component reached 25 cm/s at 16 cm above the bed at the inshore pod site and 50 cm/s at 100 cm above the bed at the FRF site. The array of 3 current meters at the offshore pod location also gave similar burst-mean alongshore current velocities, but with greater scatter. Compared to the alongshore component, cross-shore velocity induced by the same storm

was much weaker except on some occasions at the offshore site. The cross-shore components in Figures 6 and 7 were only $\frac{1}{4}$ the magnitude of their alongshore counterparts, which agrees with other shoreface observations (SWIFT *et al.*, 1985; NIEDORODA *et al.*, 1984; HEQUETTE and HILL, 1993), that alongshore velocities often dominate. Because of this alongshore velocity dominance, the storm-induced mean current remains a fairly stable direction (SSE) although the wind direction, especially during the first storm, shifted almost 90°. The cross-shore currents measured at the offshore site have more complex features comparing with their counterparts at the two inshore locations. These discrepancies are probably the result of shelf wave interference, though no supporting data are available, or because the offshore site resided in the transition zone (NIEDORODA *et al.*, 1984) where the flow structure is more complicated than that of inshore friction-dominated zone.

The setting of the burst-mean currents on this shoreface are more clearly demonstrated in Figure 9, 10 and 11 that plot the speed and direction of the currents versus speed and direction of the winds. Although the data are considerably scattered in the plots, they still demonstrate that: (a) the near-bottom current speeds are proportional to the wind speed (top panels); and (b) the current directions collapse at two main loci, 170° and 350°, and the SSE setting dominates (bottom panels). Because of the higher variations of cross-

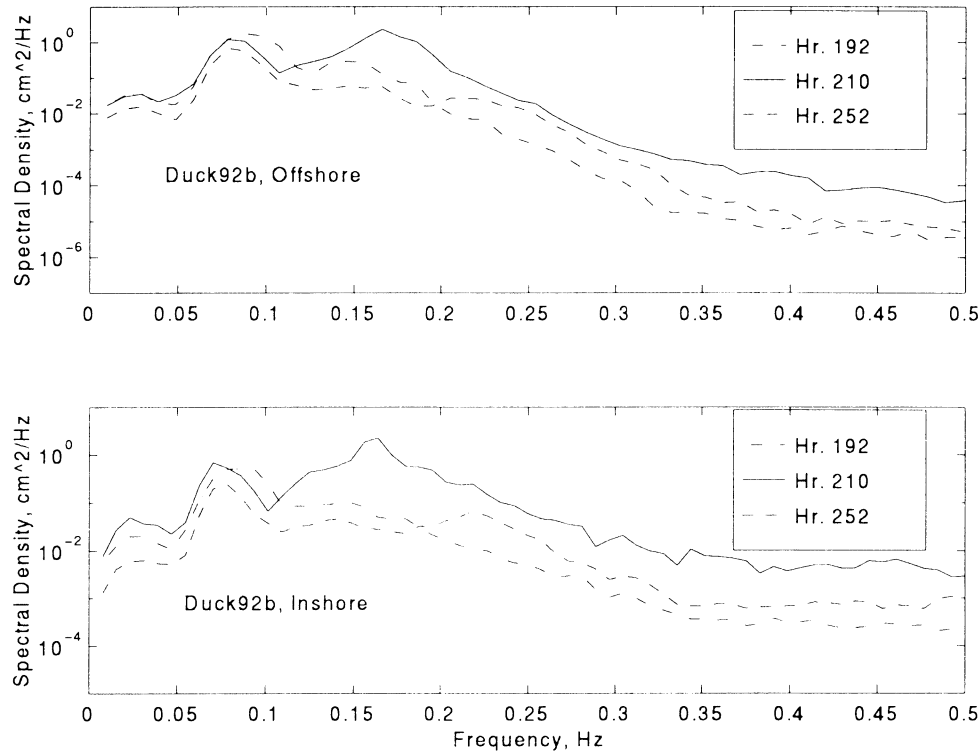


Figure 5. Power spectral density of surface waves for the three bursts that represent pre-storm, storm, and post-storm conditions during the Nov. 6 storm, at the offshore site (upper panel) and the inshore site (lower panel).

shore components at the offshore site, the plots in Figure 11 has much more scatter.

We divided the winds into 4 quadrants according to their directions (with respect to the rotated coordinates, see Figure 2), and then plotted in each quadrant the current speed versus the wind speed in Figures 12, 13, and 14. Quadrant 1 (0° – 90°) represents the events during which wind blows from the Southwest into the quadrant; and quadrant 2 (90° – 180°) through quadrant 4 (270° – 360°) are defined accordingly. The plots demonstrate that during most of the time, wind came from NE and blew into the third quadrant, *i.e.* the third quadrant has the most data points. It is more interesting to see, however, that the current speed is much more correlated to the wind speed when the latter came from the NE and NW in spite of some scatter. But this correlation does not exist in the first and fourth quadrants. In reviewing the linear regression coefficient (R^2) in each quadrant of Figures 12–14, it is obvious that quadrant 3 always has the highest R^2 value, which indicates the strongest correlation between the dependant (current speed) and independent (NE wind speed) variable. Quadrant 2 has lower R^2 values, but they are still at least an order higher than those in quadrant 1 and 4. All these observations strongly indicate the dominance of storms in characterizing the shoreface. They also substantiate that the extratropical northeasterly storms drive the largest waves and strongest, southerly setting current with downwelling cross-shore flows (WRIGHT *et al* 1986, 1994). Another

significant phenomenon in the figures is the greater third quadrant R^2 values at two inshore sites ($R^2 = 0.63$ for FRF site, and $R^2 = 0.68$ for inshore tetrapod site respectively) relative to the R^2 at the offshore site ($R^2 = 0.30$). This indicates a stronger correlation between winds and currents further inshore than offshore, and it once again support a previous statement that the inshore pod was in a friction dominated zone and the offshore pod in a transition zone. The R^2 values are by no means very high, and some errors must have been involved for the fact that the current data used to calculate the linear regression were recorded at different elevations above the bed, but they nevertheless provide a quantitative support to the theory of wind-induced shoreface currents.

CONCLUSIONS

Our limited data presented in this paper have shown that strong winds, regardless of direction, are capable of generating high seas, but only the N-NE storms produce strong alongshore current on the shoreface off Duck, North Carolina. During the 12 days deployment, two storms (hour 66–90 and 204–216, Figure 2) with strong Northeasterly winds of 10–15 m/s affected the study sites. Waves with heights of 1.7 m and periods of 5 seconds were recorded at the FRF PUV gauge. Alongshore currents reached 20 cm/s at elevation of 16 cm above the bed at the inshore site; 50 cm/s at 100 cm above the bed at FRF gage and 40 cm/s at 100 cm above the bed at

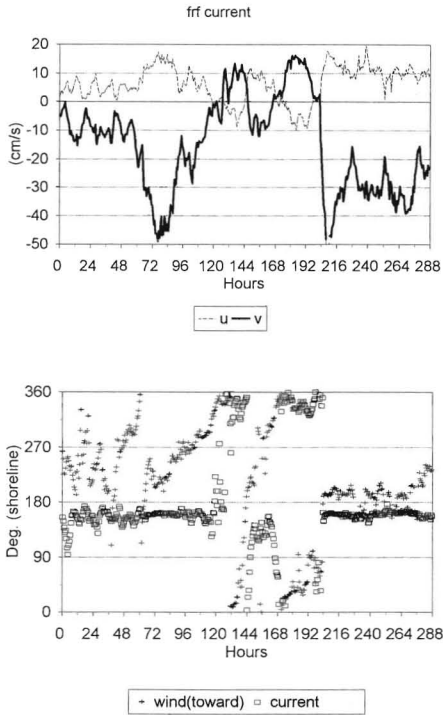


Figure 6. Cross-shore (u) and alongshore (v) current velocities at the FRF's PUV gauge. The bottom panel shows the directions of wind and current rotated relative to the shoreline. The current meter is at 100 cm above bottom.

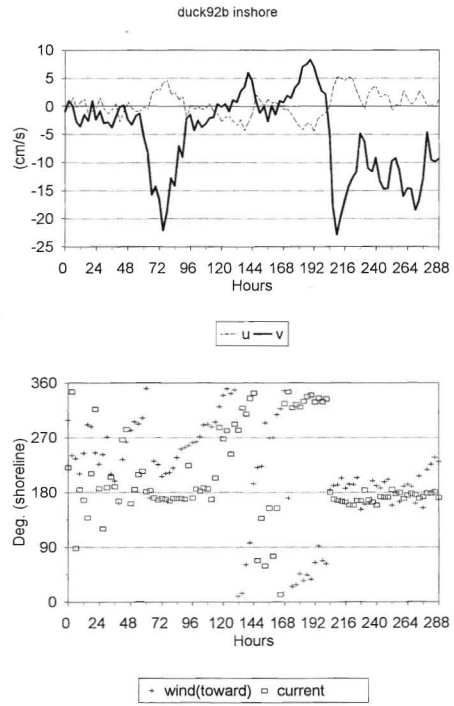


Figure 7. Cross-shore (u) and alongshore (v) current velocities at the inshore pod site. The bottom panel shows the directions of wind and current rotated relative to the shoreline. The current meter is at 16 cm above bottom.

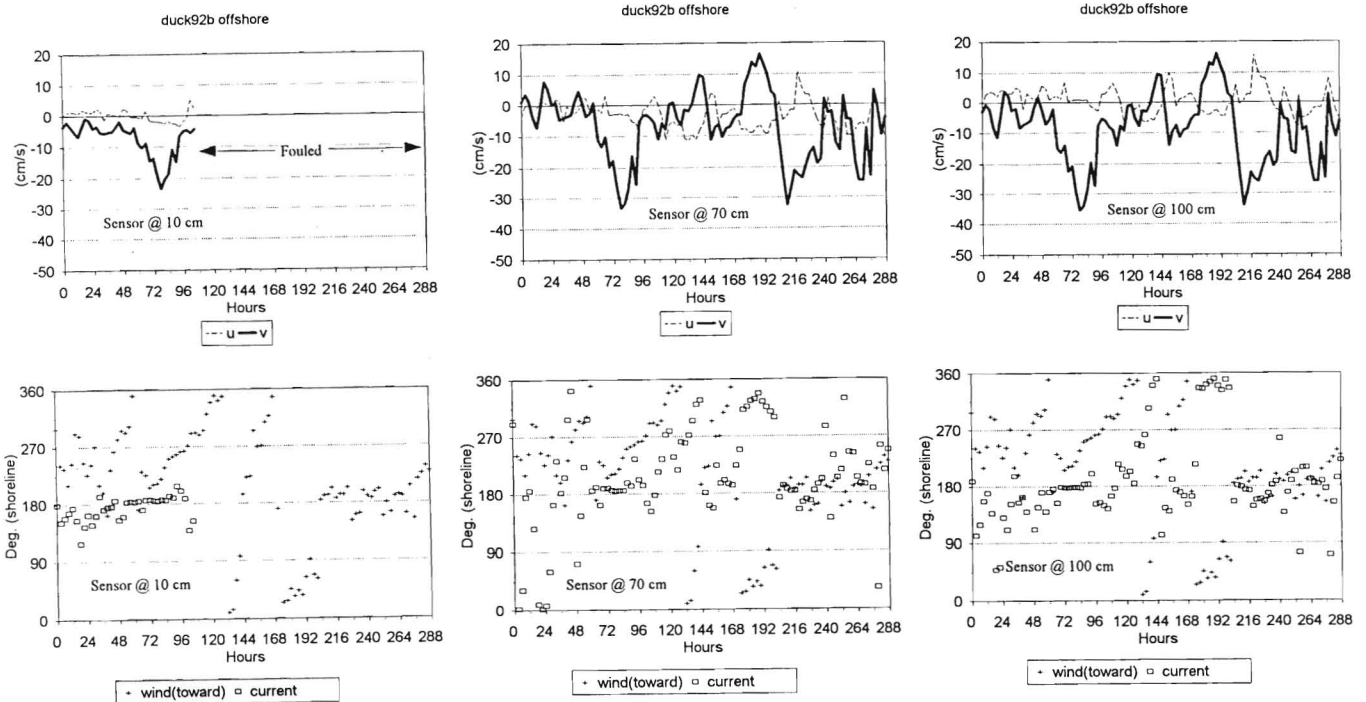


Figure 8. Cross-shore (u) and alongshore (v) current velocities at the offshore pod site. The bottom panel shows the directions of wind and current rotated relative to the shoreline. The numbers in the legend denotes the elevations (cm above bottom) of the sensors.

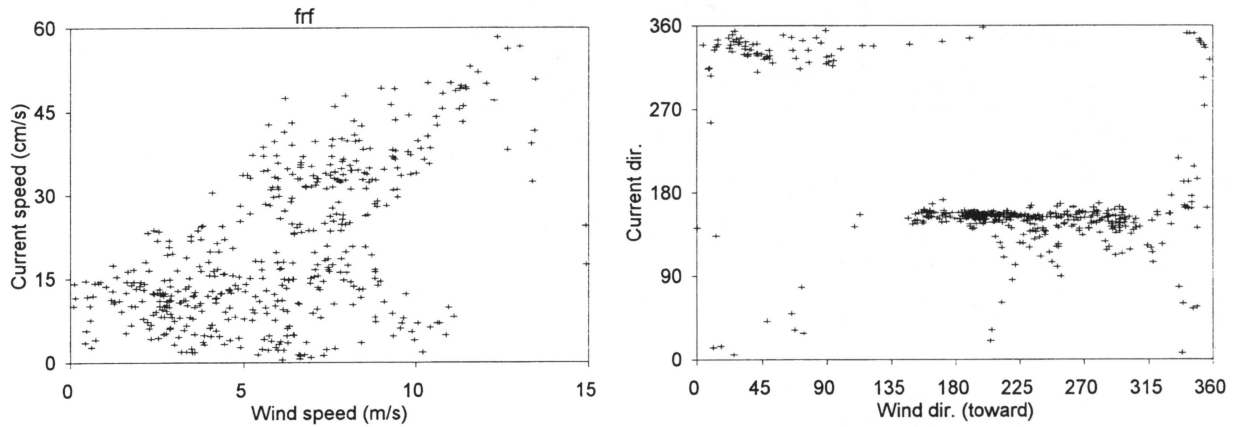


Figure 9. Plot of current speed and direction recorded at the FRF's PUV gauge vs. wind speed and direction.

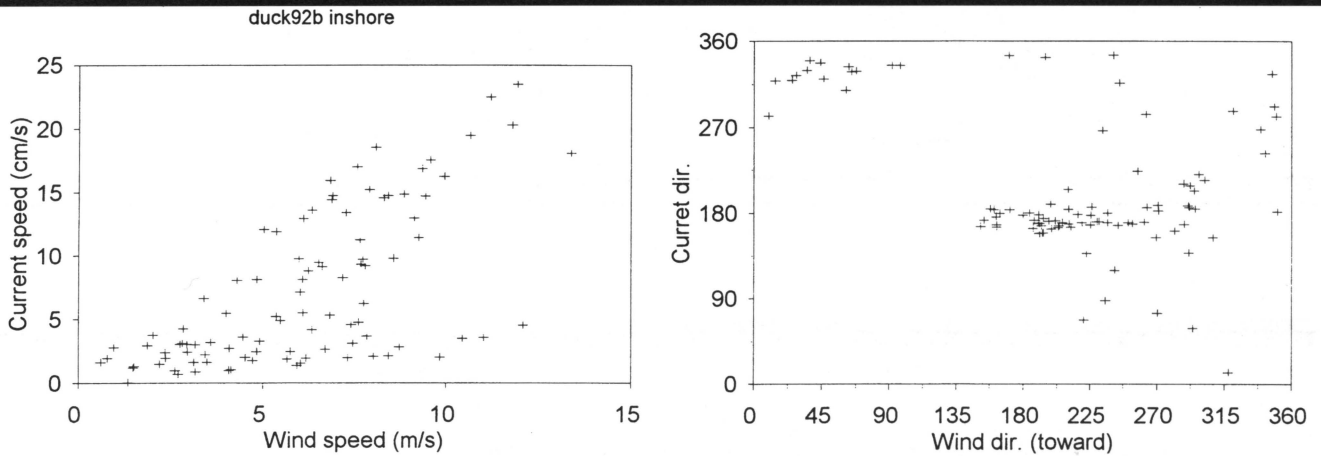


Figure 10. Plot of current speed and direction recorded at the inshore pod vs. wind speed and direction.

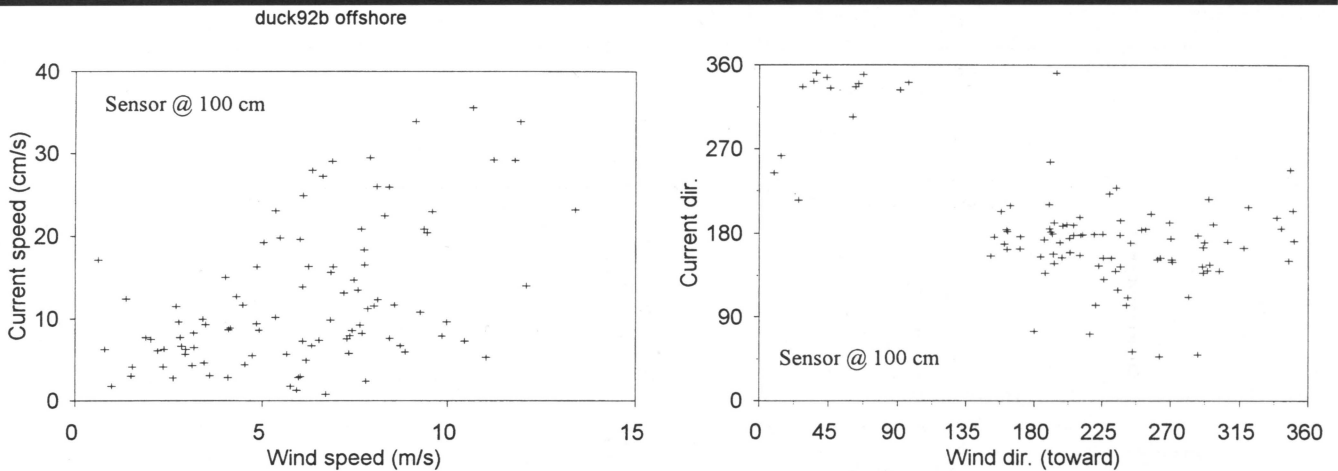


Figure 11. Plot of current speed and direction recorded at the offshore pod vs. wind speed and direction. The numbers in the legend denotes the elevations (cm above bottom) of the sensors.

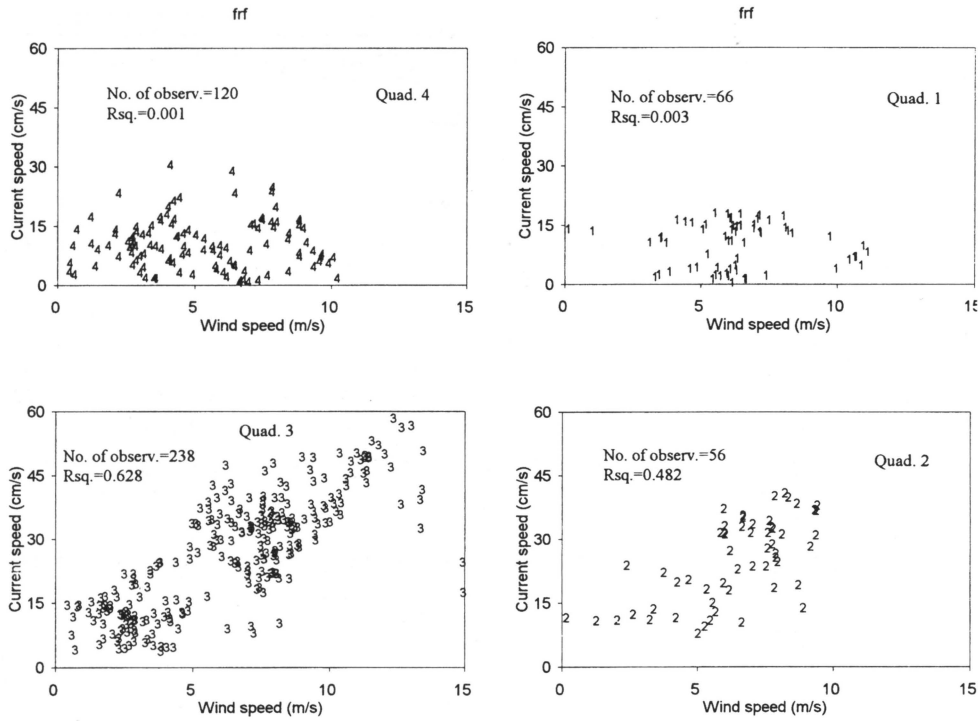


Figure 12. Same as Figure 9, but plotted in 4 different quadrants. R^2 is the linear regression coefficient.

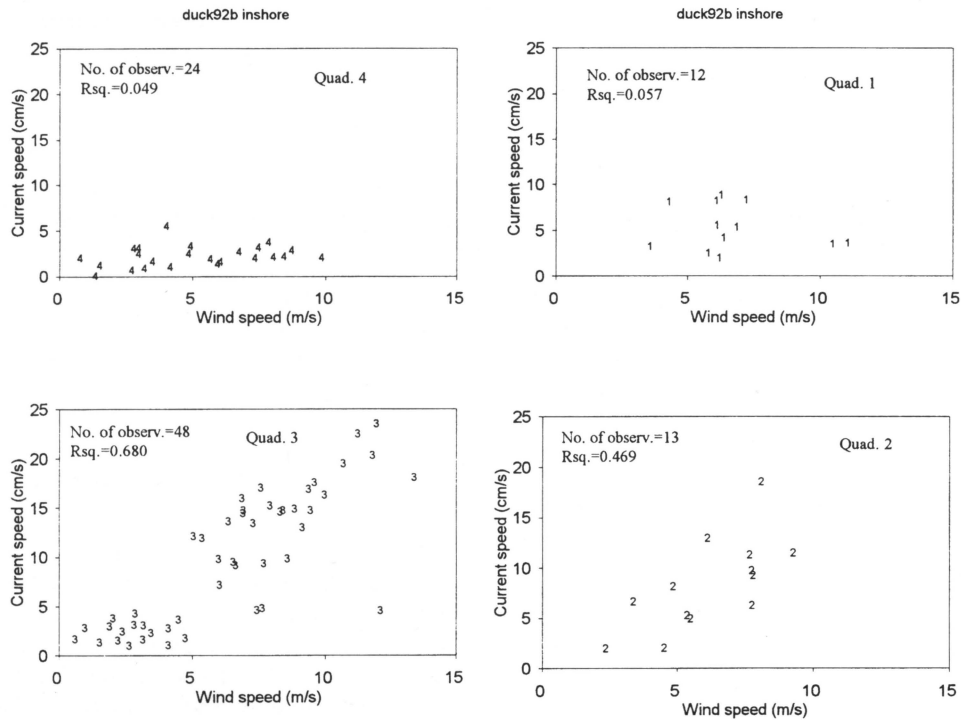


Figure 13. Same as Figure 10, but plotted in 4 different quadrants. R^2 is the linear regression coefficient.

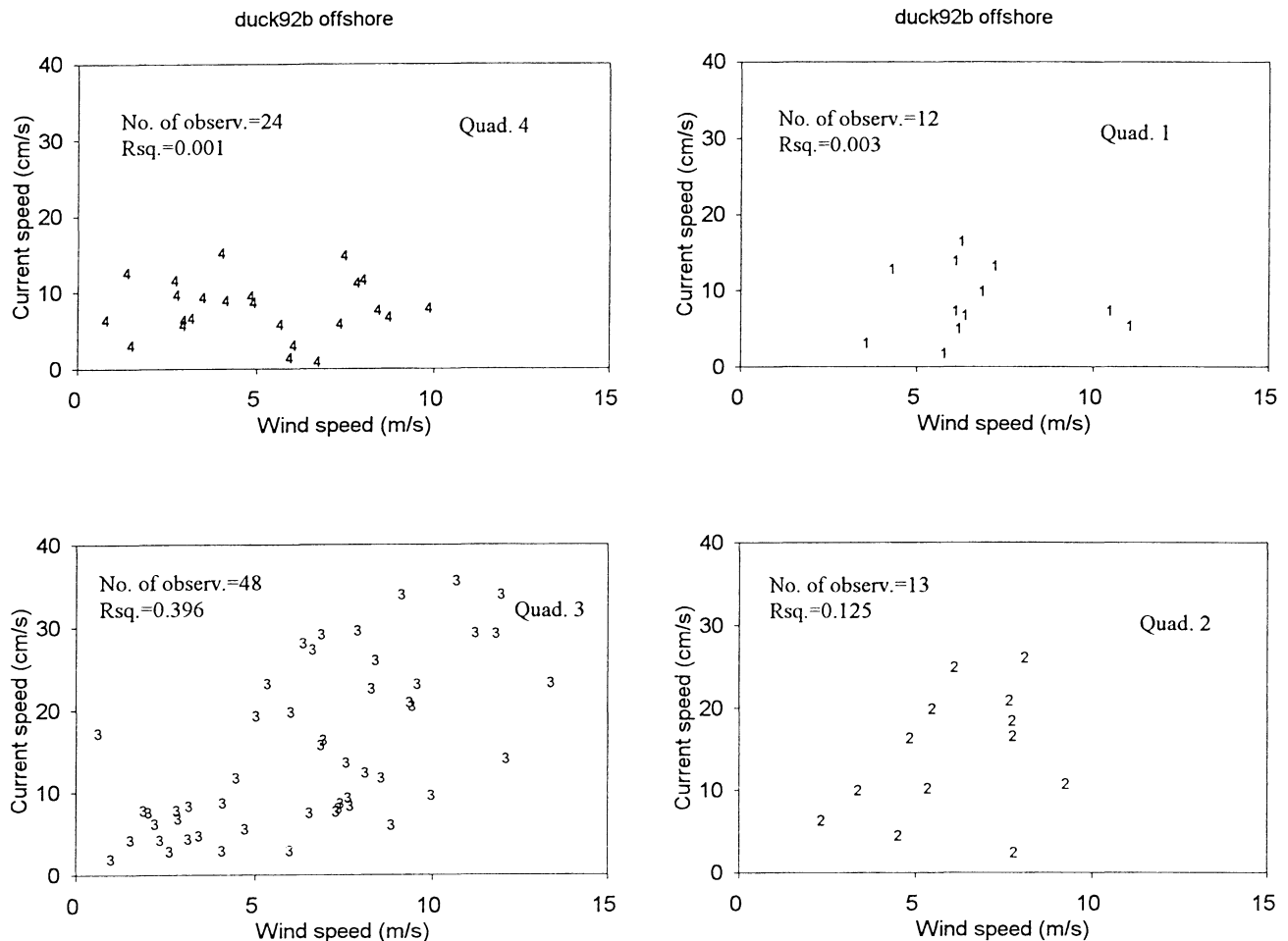


Figure 14. Same as Figure 10, but plotted in 4 different quadrants. R^2 is the linear regression coefficient. Currents measured 100 cm above bottom are used.

the offshore during the NE storms. Contrasting with the "Northeasters" was an event during Hour 105 ~ 135 in which strong winds, with speeds comparable to the Northeasterly winds, blew over 25 hours from the Southwest ~ Southeast. Although these strong winds generated substantial significant wave heights, their resultant alongshore current velocities were only 1/5 as much as the alongshore currents which occurred during the Northeasters. Therefore, the relatively high correlation between the speed of the North-Northeasterly winds and speed of wind-generated current does not exist in cases of South-Southwesterly storms. This may be attributable to the fact that, whereas downwelling-favorable "Northeasters" enhance the coastal jet (LUDWICK, 1978) and augment the buoyant coastal plume from Chesapeake Bay, upwelling favorable winds oppose the plume and do not induce jet-like responses (WRIGHT *et al.*, 1986). The near-bottom cross-shore current, unlike the alongshore counterpart, is mainly controlled by the coastal setup and setdown at the two shallower locations. The magnitude of cross-shore flow during the South-Southeasterly storm is smaller than those during the Northeasters, but the difference between speed

magnitudes among the cross-shore components is not as large as the difference among the near-bottom alongshore currents. Generally, a coastal setup (NIEDORODA *et al.*, 1985) will be developed on this shoreface, especially at the two inshore sites, which drives a seaward near-bottom cross-shore flow (downwelling) under a Northeasterly storm. Conversely, a South-Southeasterly storm will develop a coastal setdown and a shoreward near-bottom cross-shore flow (upwelling).

ACKNOWLEDGEMENT

This work has been supported by the National Science Foundation, Marine Geology and Geophysics Grant OCE-9017828. Thanks are due to Kent Hathaway and Bill Birke-meier of U.S. Army Corps of Engineers, Field Research Facility who provided the wind and FRF PUV gage data. We also thank Andrew Short and Robin Davidson-Arnott for their helpful comments. JPX acknowledges the support of Greg Stone of Louisiana State University.

LITERATURE CITED

- BOWEN, A.J., 1980. Simple models of nearshore sedimentation: beach profile and alongshore bars. In: S.B. McCANN, (ed.), *The Coastline of Canada*. Geology Survey Canada Paper, 80-10, pp.1-11.
- CSANADY, G.T., 1982. *Circulation in the Coastal Ocean*. London: Reindell, 280p.
- GUZA, R.T. and THORNTON, E.B., 1985. Velocity moments in nearshore. *Journal Waterway Port Coastal Ocean Engineering*, 111, 235-156.
- HEQUETTE, A. and HILL, P.R., 1993. Storm-generated currents and offshore sediment transport on a sandy shoreface, Tibjak Beach, Canadian Beaufort Sea. *Marine Geology* 113: 283-304.
- LUDWICK, J., 1978. Coastal currents and an associated sand stream off Virginia Beach, Virginia. *Journal Geophysical Research*, 83, 2364-2372.
- NIEDORODA, A.W.; SWIFT, D.J.P.; HOPKINS, T.S., and MA, C.M., 1984. Shoreface morphodynamics on wave-dominated coasts. *Marine Geology*, 60, 331-348.
- NIEDORODA, A.W.; SWIFT, D.J.P., and HOPKINS, T.S., 1985. The shoreface. In: R.A. DAVIS, (ed.), *Coastal Sedimentary Environments*. New York; Springer, pp. 533-624.
- SWIFT, D.J.P.; NIEDORODA, A.W.; VINCENT, C.E., and HOPKINS, T.S., 1985. Barrier island evolution, Middle Atlantic Shelf, U.S.A., Part I: shoreface dynamics. *Marine Geology*, 63, 331-361.
- WRIGHT, L.D.; BOON, J.D.; GREEN, M.O., and LIST, J.H., 1986. Response of the mid-shoreface of the Southern Mid-Atlantic Bight to a "Northeaster". *Geo-Marine Letters*, 6, 153-160.
- WRIGHT, L.D.; BOON, J.D.; KIM, S.C., and LIST, J.H., 1991. Modes of cross-shore sediment transport on the shoreface of the Middle Atlantic Bight. *Marine Geology*, 96, 19-51.
- WRIGHT, L.D.; XU, J.P., and MADSEN, O.S., 1994. Across-shelf benthic transports on the inner shelf of the Middle Atlantic Bight during the Halloween Storm of 1991. *Marine Geology*, 188, 61-77.